Selective recruitment: Evidence for task-dependent gating of inputs to the cerebellum

Ladan Shahshahani[1], Maedbh King[4], Caroline Nettekoven[1], Richard Ivry[4, 5], Jörn Diedrichsen[1, 2, 3]

1. Western Institute for Neuroscience, Western University, London, Ontario, Canada
2. Department of Statistical and Actuarial Sciences, Western University, London, Ontario, Canada
3. Department of Computer Science, Western University, London, Ontario, Canada
4. Department of Psychology, University of California, Berkeley, CA, USA
5. Helen Wills Neuroscience Institute, University of California, Berkeley, CA, USA

* To whom correspondence should be addressed: Ladan Shahshahani, Western Institute for Neuroscience, Western Interdisciplinary Research Building, Western University, N6A 5B7, London, ON, CA. Email: lshahsha@uwo.ca

Contributions: L.S. and J.D. originally conceived of the project. L.S. and J.D. designed the experiment. L.S. collected the data. L.S. performed the analyses. L.S., J.D., C.N., M.K., and R.I. wrote the manuscript. All authors discussed the results and contributed to the final manuscript.

Acknowledgements: This work was supported by the Canadian Institutes of Health Research (PJT 159520 to J.D.), the Canada First Research Excellence Fund (BrainsCAN to Western University), and the National Institute of Health (NS092079, NS105839 to R.B.I.). Thanks to Da Zhi for providing cerebral cortical parcellations.

Competing Interests: R.I. is a co-founder with equity in Magnetic Tides, Inc. The other authors declare no competing interests.

Abstract

While fMRI studies have documented cerebellar activity across a wide array of tasks, the functional contribution of the cerebellum within these task domains remains unclear. Here we present a new framework to address this problem, asking if neocortical inputs to the cerebellum are gated in a task-dependent manner. We tested this idea in the context of finger movements, where the integrity of the cerebellum has been shown to be essential for the coordination of rapid alternating movements but not grip force generation. While neocortical and cerebellar activity both increased with increasing speed and force, the changes in cerebellar activity associated with speed were larger than predicted by an optimized cortico-cerebellar connectivity model. This suggests a task-specific recruitment of the cerebellum through gating of information between the cerebellum and neocortex. More generally, this framework offers a new approach to identify cerebellar contributions to function using fMRI.

Significance statement

Previous functional imaging studies have shown the cerebellum is activated across a large range of tasks. However, drawing specific inferences about cerebellar function from this work has been difficult because activation patterns in the cerebellum are strongly constrained by its anatomical connectivity with the neocortex. As activity in the neocortex increases, corresponding changes should be expected in the cerebellum, regardless of whether the cerebellum is functionally involved in the task or not. We present

a new framework to address this problem, comparing cerebellar activations with that predicted by a task-general cortico-cerebellar connectivity model. Applying this approach in the motor domain, we show that the input to the cerebellum is preferentially upregulated for the coordination of rapid, alternating finger movements.

Introduction

More than 30 years of neuroimaging has revealed that the human cerebellum is activated in a broad range of tasks including motor (Spraker et al., 2012), language (Petersen et al., 1989), working memory (Marvel & Desmond, 2010), attention (Allen et al., 1997), social (Van Overwalle et al., 2015), and visual cognition (Diedrichsen et al., 2019; Van Essen et al., 2011). The presence of cerebellar activity has often been taken to indicate that the cerebellum plays a specific functional role in these tasks.

However, there is an important problem with this line of reasoning. The cerebellar BOLD signal is dominated by mossy fiber input with very little contribution from the output of the cerebellar cortex, the activity of Purkinje cells (Alahmadi et al., 2015, 2016; Gagliano et al., 2022; Mapelli et al., 2017; Mathiesen et al., 2000; Thomsen et al., 2004). The mossy fiber inputs, in turn, arise from a wide array of neocortical areas, including prefrontal and parietal association cortices. This has been demonstrated directly through viral tracing studies in non-human primates (Kelly & Strick, 2003), and indirectly through resting-state functional connectivity (rs-FC) analysis in humans (Buckner et al., 2011; Ji et al., 2019; Marek et al., 2018; O'Reilly et al., 2010). The existence of these anatomical connections certainly argues for a prominent role of the human cerebellum in cognition in general (Leiner et al., 1986; Strick et al., 2009). However, an increase in the cerebellar BOLD signal need not indicate that the cerebellum is making a functional contribution to that specific task: Cerebellar activity could simply reflect the automatic transmission of neocortical activity through fixed anatomical connections. Indeed, if all cerebellar BOLD activity can be perfectly explained by its fixed connectivity with the neocortex, then it would be hard to learn anything specific about cerebellar function from fMRI studies.

But, what if the neocortical input to the cerebellum was amplified when a specific contribution from the cerebellum was required? We refer to this idea as the *selective recruitment* hypothesis. Such task-dependent gating would make evolutionary sense, given the substantial metabolic cost of granule cell activity (Attwell & Iadecola, 2002; Howarth et al., 2010). In the current study we test the selective recruitment hypothesis in the motor domain, where clinical studies provide a strong *a priori* hypothesis: Patients with cerebellar damage consistently show impairments in performing rapid alternating movements, a symptom called dysdiadochokinesia (Hallett et al., 1991; Mai et al., 1988). In contrast, these patients are generally able to exert grip forces comparable to healthy controls (Mai et al., 1988). This clinical dissociation suggests that the computations required to produce fast alternating finger movement depend more on the cerebellum than those required to modulate grip force.

To test whether this differential dependency leads to selective recruitment of the cerebellum during rapid alternating movements, we employed a task involving alternating finger presses (Fig. 1a). Starting at a baseline level of 1Hz and 2.5N, we either increased the force of the required finger movements, or their speed (Fig. 1b). We expected that increases in speed and force would both result in an increased BOLD signal in the neocortex and cerebellum (Spraker et al., 2012). The selective recruitment hypothesis predicts that increases in cerebellar BOLD will be greater for increases in tapping speed compared to increases in finger force output, even when the neocortical activity is matched between conditions (Fig 1c).

This comparative approach requires the definition of a neocortical region that can serve as a control for each cerebellar region of interest. While rs-FC studies (Buckner et al., 2011; Ji et al., 2019; Marek et al., 2018) have identified a system of paired neocortical and cerebellar networks, the 1:1

mapping featured in these networks glosses over the possibility that cerebellar regions may receive input from more than one neocortical region. To test for cortico-cerebellar convergence, we recently developed a series of connectivity models (King et al., 2022) optimized to predict cerebellar activity patterns from neocortical activity patterns across a wide array of tasks. Models that allowed graded input from multiple neocortical regions predicted cerebellar data better than models that allowed input from only a single region. Thus, we used these models here to obtain predictions of cerebellar activation, assuming that functional connections are fixed (i.e., task-invariant). These predictions serve as a baseline against which we test the idea of selective cerebellar recruitment.

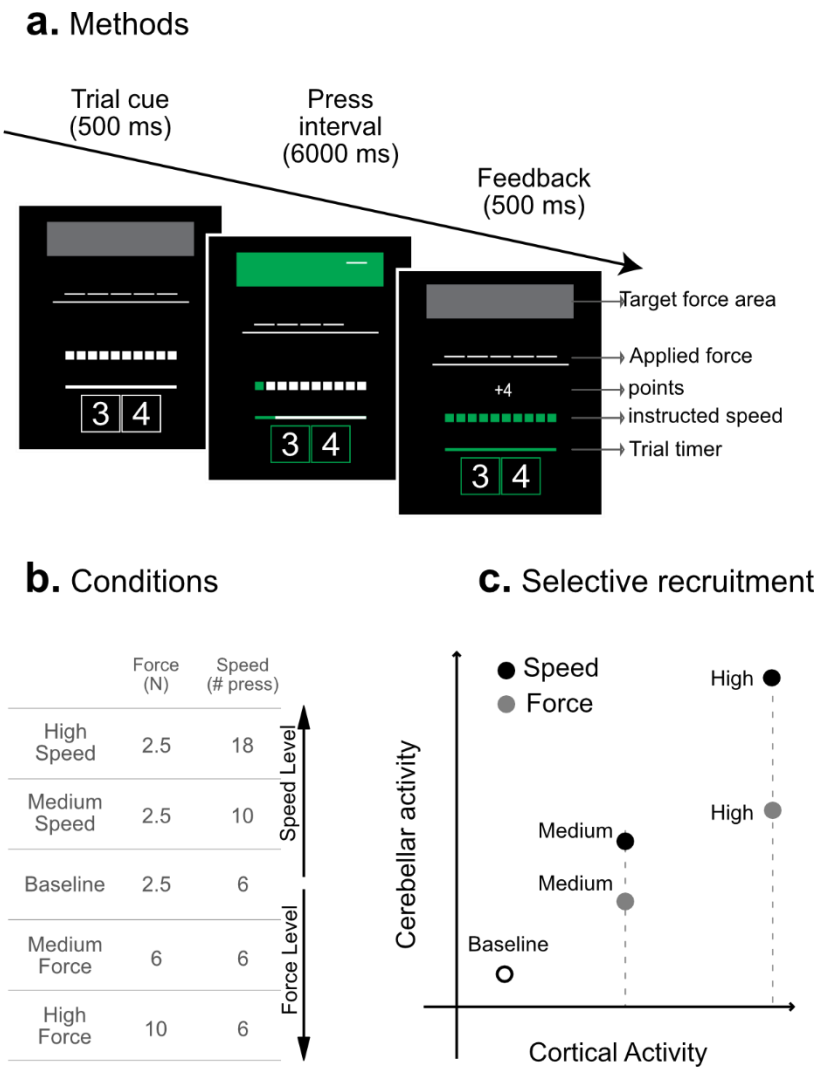

	Force (N)	Speed (# press)	
High Speed	2.5	18	Speed Level
Medium Speed	2.5	10	
Baseline	2.5	6	
Medium Force	6	6	Force Level
High Force	10	6	

Figure 1. Alternating finger tapping task and expected results from selective recruitment. a) Timeline of events in a single trial. Cues specified the target speed and force level. During the press interval, participant alternatively tapped the middle and ring finger. Reward feedback (e.g., +4) was based on their performance. **b)** The 5 force-speed combinations. The baseline condition was performed at the lowest levels of force and speed. For the other conditions, either the target force or speed increased. Speed indicates the number of presses to be produced within a 6 s interval. **c)** Expected results for the selective recruitment hypothesis: For approximately matched neocortical activity levels (x-axis) in the medium and high conditions (dashed lines), cerebellar activity (y-axis) is expected to be greater for increases in speed compared to increases in force.

Results

Behavioral performance in the scanner

The group-averaged peak forces and number of taps over the 6s interval are presented in Table 1. Overall, participants performed as instructed. For all individuals the mean force for each condition was within 80-120% of the target force and the mean number of taps was ±2 of the target number. Trials in

which the participant did not perform at the instructed speed (TOO FAST), produce the instructed number of presses (±2) in time, or tapped with the wrong finger were considered errors. The high error rate for the baseline condition reflects the fact that some of the participants had difficulty maintaining the relatively slow rate, completing the 6 taps in less than the minimum interval of 4 s. Error trials were excluded from the mean performance data and from the imaging analysis.

Condition	Average force (N)	Number of taps in 6s	Error rate (%)
High Speed	2.93 ± 0.48	17.72 ± 0.84	5 ± 0.21
Medium Speed	2.84 ± 0.45	10.12 ± 0.44	1 ± 0.12
Baseline	2.80 ± 0.41	6.32 ± 0.8	15 ± 0.36
Medium Force	6.10 ± 0.49	6.04 ± 0.2	4 ± 0.18
High Force	9.73 ± 0.66	6.04 ± 0.2	2 ± 0.13

Table 1. Mean and standard deviation of executed force, speed, and error rate for each condition across subjects.

Increased activation in neocortical and cerebellar motor networks

Given that our task involved right-hand movements, we expected to observe prominent activation in the hand areas of left (contralateral) M1 and S1. This was indeed the case (Fig. 2). Compared to baseline, the combined M1/S1 ROI showed a significant increase in activation averaged over medium and high force levels (Fig. 2a, $t_{15} = 8.45$, $p = 4.34\times10^{-7}$), as well as for the medium and high-speed conditions (Fig. 2c, $t_{15} = 5.44$, $p = 6.87\times10^{-5}$). Similarly, activity in the right anterior and posterior motor areas of the cerebellum increased with increasing force (Fig. 2d, $t_{15} = 9.87$, $p = 5.93\times10^{-8}$) and speed (Fig. 2f; $t_{15} = 4.98$, $p = 1.62\times10^{-5}$). These results replicate the findings from previous studies, showing that activity in the cerebellar hand motor areas are sensitive to parametric variation of force (Spraker et al., 2012) and speed (Jäncke et al., 1999).

Visual inspection of Figure 2 suggests that the cerebellar signal is more strongly modulated by variation in speed than force. However, we cannot use this to infer any preferential functional role for the cerebellum: It is possible that the BOLD activity in the associated neocortical areas is also more sensitive to variation in speed, and that the cerebellar changes simply reflect these neocortical changes.

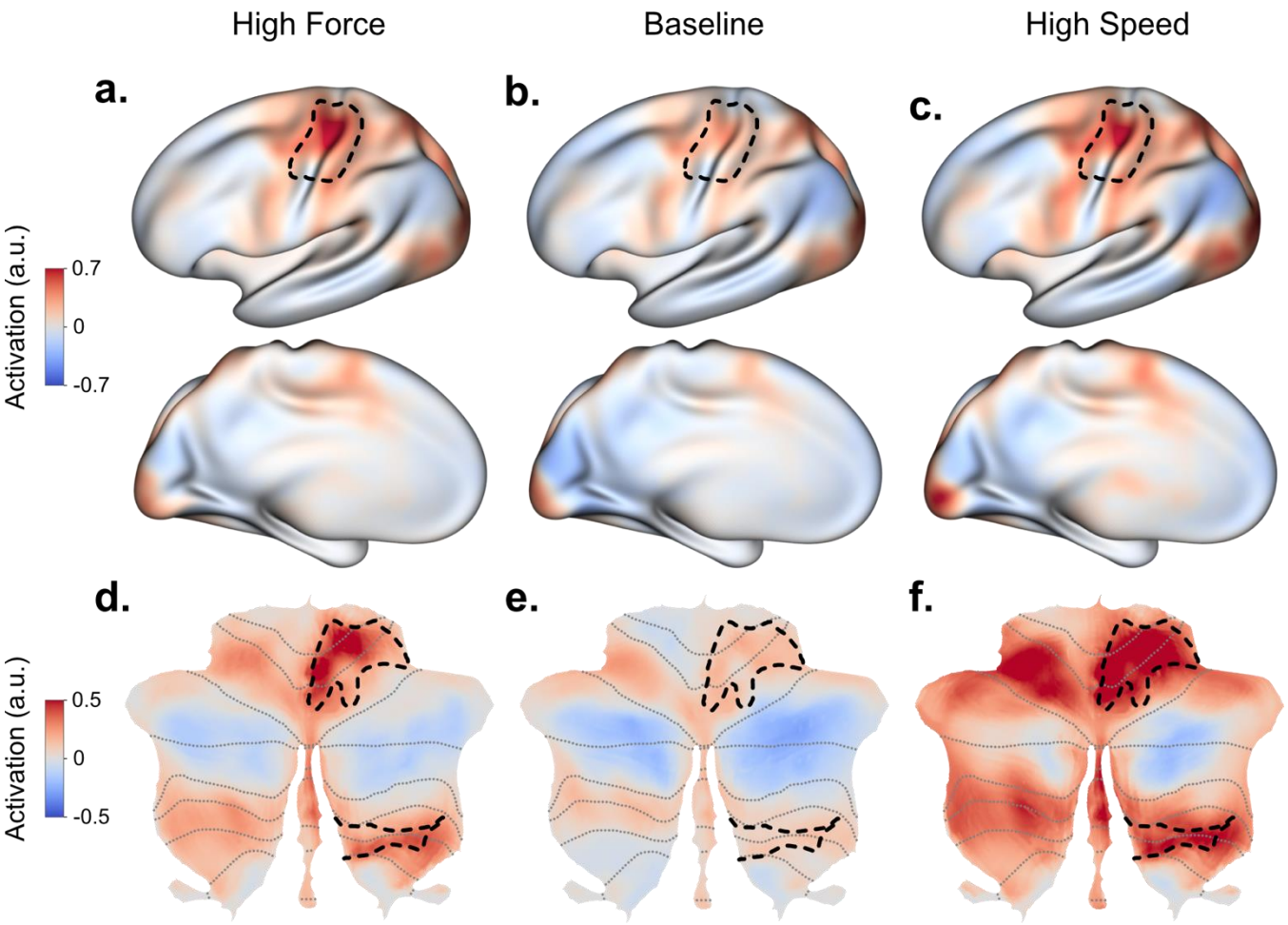

Figure 2. Activation in the cortico-cerebellar motor network compared to rest. Activity maps are shown for high force (left), baseline (middle), and high speed (right) conditions. High levels of force and speed were chosen to visualize the overall trend in activity increase with increasing force and speed. (**a-c**) Lateral and medial surface of the left hemisphere with the hand area of M1 and S1 indicated by a black outline. (**d-f**) Flat map of the cerebellum with anterior and posterior motor areas outlined by black dotted lines. The motor hand area of the cerebellum was selected from the functional parcellation introduced in (King et al., 2019).

ROI-based comparison of neocortical and cerebellar hand regions

The preceding discussion makes clear that we need to evaluate the change in cerebellar activity within the context of the activity in neocortical regions that provide input to that cerebellar region. To do so, we focused on the right-hand area of the human cerebellum, as defined by a recent functional parcellation (King et al. 2019). To select the corresponding neocortical area, we assumed in this initial analysis that the contralateral sensorimotor areas of the neocortex are the **only** regions that provide input to the cerebellar hand area. To define the contralateral M1 / S1 hand ROI, we used a cyto-architectonic atlas (see Methods, Fig. 2). The observed activation for each condition was averaged in the neocortical/cerebellar ROIs. As expected, activation in both cerebellar and neocortical motor areas

increased with force and speed (Figure 3A). However, the pattern across these two variables was different for the neocortex and cerebellum. For example, in the neocortex, activity in the high-speed condition lay between the medium and high force conditions whereas in the cerebellum, activity in the high-speed condition was larger than in either force condition. Thus, the cerebellar activity was not simply a monotonic function of the neocortical activity.

A different way of showing this is to correct the cerebellar activity for differences in neocortical activity. We fit a linear model between these two variables for each participant (average R^2 = 0.58, SE= 0.01). We then computed the residuals of this linear model for each condition. These residuals indicated whether the cerebellum was more or less activated than expected given a fixed connectivity model. The signed residuals averaged for the speed conditions were significantly higher than those for the force conditions (t_{15} = 3.01, p = 8×10^{-3}). Thus, this initial analysis indicates that, in response to an increase in movement speed, the cerebellar activity increased to a greater degree than expected from the increases in neocortical activation.

Model-based comparison of predicted and observed cerebellar activity

One limitation with our initial analysis is that we assumed that only M1/S1 provides input to the hand area of the cerebellum. Is it possible that the higher activity in the cerebellum was caused by fixed inputs from the additional neocortical areas?

The activation patterns for speed and force conditions were not completely matched: Increases in speed tended to lead to more widespread activations in secondary motor areas than increases in force. Given this difference, the observed differences in cerebellar activity may be a result of additional fixed inputs from premotor and supplementary motor areas, rather than evidence in support of selective recruitment.

To evaluate this hypothesis, we utilized a model of cortico-cerebellar connectivity derived from a large task battery (King et al., 2022). The best-fitting model indicated that cerebellar voxels receive convergent inputs from multiple neocortical areas. The connectivity weights of this model averaged across all voxels in the right cerebellar hand ROI are shown in Figure 3b (Ridge regression, see *Methods*). As can be seen, input weights are not limited to contralateral M1 and S1, but also include premotor and supplementary motor regions. To determine whether these additional inputs account for the observed differences in cerebellar activity between conditions, we used the connectivity weights from the model to predict the cerebellar activity patterns for each participant and condition from the individual's neocortical activity patterns.

Using the connectivity model, the predicted and observed cerebellar activations levels averaged for the selected cerebellar ROI (Fig. 3c), were more closely matched (average R^2 = 0.83, SE = 0.07). Nonetheless, the predicted task-specific deviations from the predictions remained. After accounting for the small differences in predicted activity, the average signed residual for the two speed conditions was significantly higher than for the force conditions (t_{15} = 3.21, p = 5×10^{-3}). In summary, the increases in cerebellar activity for speed outstripped the activity increases for force, even if we accounted for the activity in the likely neocortical input regions.

Alternative connectivity models

We recognize that our results are dependent on the connectivity model used to predict cerebellar activity. To explore the robustness of our results, we considered two other cortico-cerebellar-connectivity models, one based on a winner-take-all algorithm in which the cerebellar input is restricted to neocortical area with the highest correlation, and a lasso regression model that allows for some convergence of neocortical input (King et al., 2022). We note that, while these models did not perform as well as the

Ridge model in predicting cerebellar activity patterns, each provided reasonable predictive accuracy. When these connectivity models were applied to the current data set, we obtained a similar pattern of predictive deviations: The signed residuals were significantly higher for conditions with higher speeds (winner-take-all: $t_{15} = 2.5$, $p = 2\times10^{-2}$, lasso regression: $t_{15} = 3.29$, $p = 5\times10^{-3}$, averaged over medium and high levels).

Voxel-wise analysis across the cerebellum

The previous analyses focused on a specific region of the cerebellum, the right-hand motor areas. These analyses do not address whether there are other cerebellar regions that also show higher-than-predicted activity for increasing speed, or whether there are cerebellar regions that show the opposite pattern with higher-than-predicted activity for increasing force. To address this, we tested for violations of the prediction of the Ridge connectivity model in each cerebellar voxel. Figure 4c shows the difference between the observed and predicted activity, displayed as a statistical map of the speed vs. force comparison. Voxels that showed higher speed sensitivity (relative to neocortical activity) were found in anterior and posterior cerebellar motor regions. Additionally, we found higher than predicted activity in default-mode regions of left crus I + crus II, as well as in language-related areas of the right crus I and crus II.

Importantly, we found no cerebellar regions in which the residuals for the high force conditions were greater than those for the high-speed conditions. Thus, the results show that deviations from our task-invariant connectivity model selectively arise when the rate of alternating finger movements increases and that this effect is primarily observed in task-specific areas of the cerebellum.

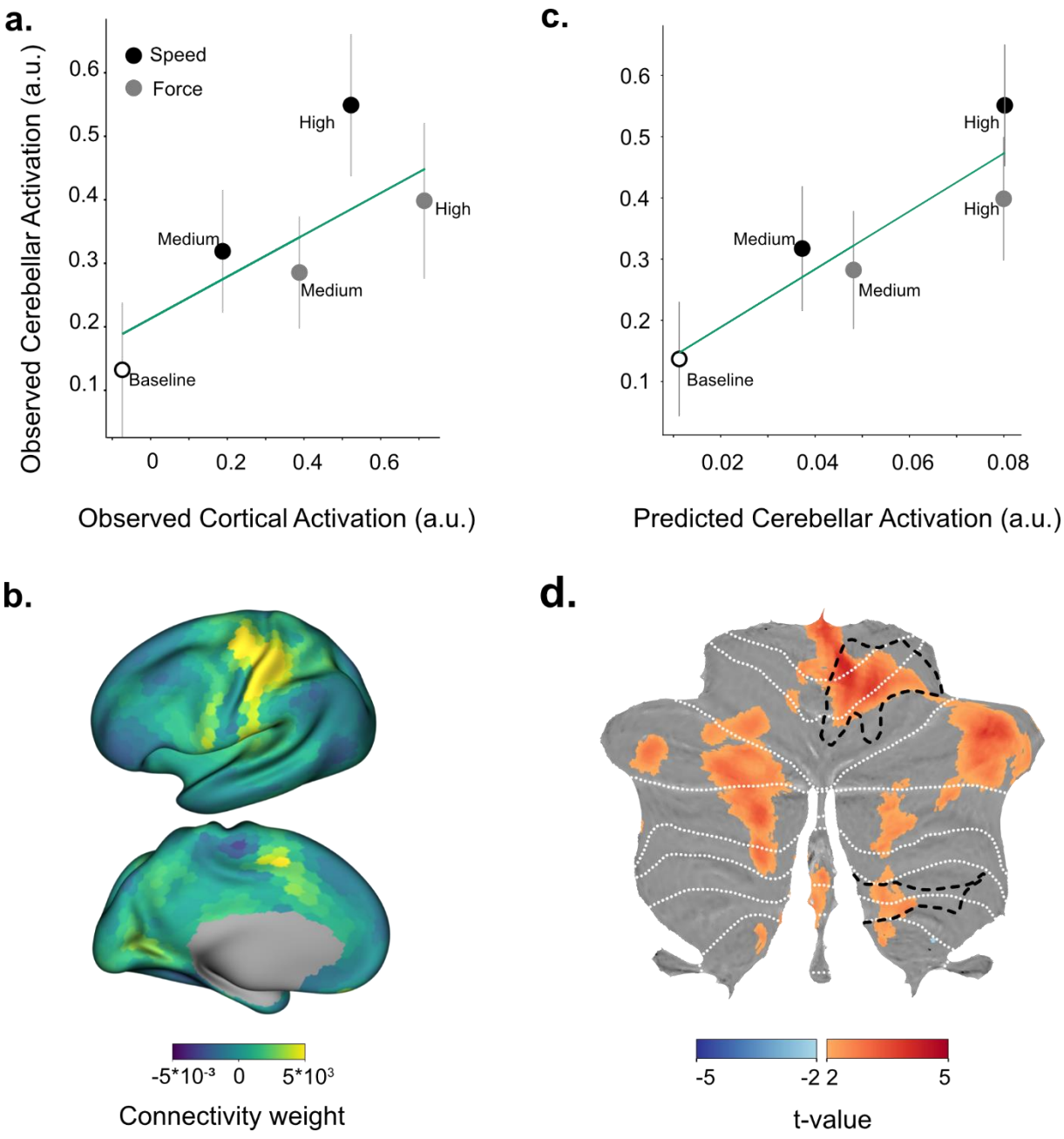

Figure 3. Selective recruitment of cerebellum for fast alternating finger movements. a) Average BOLD activity in the right-hand cerebellar ROI (y-axis) plotted against activity in the contralateral M1/S1 regions (x-axis). Error bars indicate standard error of the signed residuals from the linear regression model within each participant (see Methods). **b**) Connectivity weights from a group-level connectivity model (Ridge regression) for the cerebellar motor ROI (from King et al., 2022). **c)** Average observed cerebellar activation (y-axis) plotted against average prediction from the connectivity model (x-axis). The signed residuals were significantly higher for the speed compared to the force conditions. Note that the predicted activations for high levels of force and speed are closely matched using the connectivity model. **d)** Thresholded map of t-values testing where the residuals for the speed conditions were greater than the force conditions. No cerebellar voxels showed more positive residuals for the force compared to the speed conditions (blue, note that the t-tests were two-tailed).

Discussion

Functional neuroimaging studies have shown that the human cerebellum is activated across a broad range of task domains. However, drawing functional inferences from these activations is limited

by the fact that the BOLD signal in the cerebellar cortex is largely dominated by mossy-fiber input (Alahmadi et al., 2015, 2016; Gagliano et al., 2022; Mapelli et al., 2017; Mathiesen et al., 2000; Thomsen et al., 2004, 2009), which mainly carries incoming information from neocortex. Thus, it is difficult to draw inferences about the engagement of the cerebellum by considering cerebellar BOLD activity in isolation; this signal may simply reflect information transmission through fixed anatomical connections.

Our current experiment clearly illustrates this problem. We found highly significant increases in the cerebellar BOLD signal for increases in force. This observation could be interpreted as evidence that the cerebellum is involved in the processes required to generate higher forces. However clinical studies have shown that cerebellar pathology results in the impaired ability to produce fast alternating movements, but does not impact maximal force generation (Mai et al., 1988). Thus, consideration of the changes in the cerebellar BOLD in response to force would not align with this clinical dissociation.

In the present study, we introduce a more stringent criterion to infer functional involvement of the cerebellum: Rather than focusing on activation per se for a given task, the emphasis should be on whether the cerebellar area exhibits a signature of what we refer to as selectively recruitment. To establish selective recruitment, we need to interpret cerebellar activity in the context of the simultaneously occurring neocortical activity. Specifically, the observed cerebellar activity should be compared to the activity that would be expected if neocortical activity was transmitted over fixed, task-invariant connections.

To enable this comparison, we drew on a cortico-cerebellar connectivity model (King et al., 2022) that was optimized to predict cerebellar activity based only on neocortical activity patterns across a wide array of tasks. This connectivity model provides a carefully constructed null hypothesis of the expected cerebellar activity given a pattern of neocortical activity. Note that this prediction takes into account that some functional networks, such as the fronto-parietal and salience networks, occupy a relatively larger area of the cerebellum than of the neocortex (Marek et al, 2018, Buckner et al., 2011), and that there will be variation in convergence across the cerebellar cortex. As shown in our previous study (King et al. 2022), this model provides a good prediction of cerebellar activity across a broad range of tasks, including those not used in developing the model, confirming that a large proportion of the observed variation of cerebellar activity across tasks can be accounted for by fixed functional connections between neocortical and cerebellar regions.

Here we ask if there are systematic deviations from these predictions. Specifically, the selective recruitment hypothesis proposes that neocortical input is upregulated when the cerebellum is required for a task (and/or downregulated when it is not). If this was true, we should be able to detect specific violations of the task-invariant connectivity model. The current results showed selective recruitment of the cerebellum during rapid alternating finger movements: Activity in the cerebellar hand area increased **more** when increasing speed as compared to force. Importantly, this dissociation was observed even when the activity in the neocortical hand areas was approximately matched across these conditions. These results provide clear evidence for task-dependent gating (Cole et al., 2021), a signature we take to indicate tasks that are dependent on cerebellar computations.

There are a number of possible neural mechanisms that could underlie such task-dependent regulation. First, gating may occur in the pontine nuclei, which integrates descending signals from different areas of the neocortex with feedback signals from the cerebellum (Schwarz & Thier, 1999). The cellular properties of pontine neurons makes them ideally suited to gate input signals in a state-dependent manner (Schwarz et al., 1997). Second, gating could be achieved via modulation within the granule cell layer itself, perhaps by recurrent loops involving inhibitory Golgi cells (Maex & Schutter, 1998). Finally, gating may already occur in the neocortex: A recent study (Park et al., 2022) showed more recruitment of neocortical neurons that project to the pons when controlling the spatial aspects of joystick

manipulation, and more recruitment of neurons that project intra-cortically or to the striatum when controlling movement amplitude. Because the neocortical BOLD signal reflects the activity of both neuronal populations, pontine-projecting neurons may be more engaged during fast alternating movements, even though the fMRI activity is the same as during the production of high forces. Whichever combination of mechanisms is responsible for our observed effect, task-dependent gating of inputs to the cerebellum would be highly adaptive from a metabolic standpoint (Attwell & Iadecola, 2002), such that the costly mossy-fiber system is most activated when cerebellar computation is required.

One drawback of our new approach is that it heavily depends on the connectivity model that is used to make predictions about the expected cerebellar activity. Here we considered a range of models, starting from a simple one-to-one connectivity model that only uses the most likely neocortical input area (in the present study, M1/S1) to full connectivity models that were optimized to predict cerebellar activity across a large array of tasks. The latter models allow for the convergence of inputs from multiple neocortical areas and provide significantly better predictions than a simple one-to-one pairing of cerebellar and neocortical areas (King et al., 2022). Similar to our earlier work, the full connectivity model provided better predictions of the current data than the simple ROI approach. These findings emphasize the importance of using a model that approximates the true cortico-cerebellar connectivity as closely as possible. This will be especially important for cognitive regions in lobules VII, which appear to receive input from an even wider array of regions (King et al., 2022).

A second limitation of our approach is that the connectivity model as currently constructed does not predict the absolute level of cerebellar activity, but rather activity for one condition relative to other conditions. This limitation arises from the fact that the absolute magnitude of the BOLD signal in the cerebellum depends on many measurement-related factors, which may differ between the study used to estimate the connectivity model and a subsequent experiment that draws on this model. To address this uncertainty, we fit the average numerical relationship between neocortical and cerebellar activity for each participant separately. Thus, our approach relies on the comparison to a control condition (here force generation) that activates similar neocortical regions but does not (or to a lesser degree) rely on the cerebellum. From this we can conclude that the input gain in the speed condition was higher than in the force condition. Whether this was achieved by a specific upregulation in the speed condition, or a downregulation in the force condition is unclear.

This leads to question of why cerebellar activity, if it was functionally not important for pressing harder, increased in the force condition at all. One explanation is that the cerebellum is, alongside neocortex, functionally involved in the force conditions, perhaps for accurately maintaining the target force levels (Mai et al., 1988), or for avoiding finger-to-finger enslaving effects that emerge at high force levels (Brandauer et al., 2012). We designed our force task to have minimal force accuracy (accepted forces range from 80% to 120% of the target force) and individuation requirements, with the idea that satisfactory task performance could be achieved with minimal cerebellar involvement during force processing given the clinical literature.

A more likely explanation is that the force-related increases in cerebellar activity occur because neural gating is not complete: Neocortical inputs to the cerebellum are attenuated when cerebellar function is not required but are not entirely shut down. Given the diversity of neocortical functions combined with the uncertainty about which function will rely on cerebellar computation, a partial task-invariant information transmission to the cerebellar cortex certainly seems functional. If gating is indeed incomplete, then we should expect to observe increases in cerebellar activity (as here in the force condition) even when the cerebellum makes minimal contributions to task performance.

In summary, we outline here a new approach for using fMRI data to evaluate hypotheses about cerebellar function. Rather than just showing that the cerebellum is activated for a specific task, we apply a more stringent criterion, asking if the cerebellum is *more* activated than predicted by a task-invariant

connectivity model. Tasks that meet this criterion, especially when compared to control conditions in which cerebellar activity is well predicted by the connectivity model, will provide strong evidence that cerebellar computations are important for those tasks. Our results provide an important first validation of this approach showing that fMRI activity, and therefore likely cortico-pontine-cerebellar input, is modulated in a task-dependent manner. As expected from clinical observations, we showed that the cerebellar hand area is selectively more activated for increases in speed relative to increases in force. The framework developed here in the motor domain where we had strong *a priori* expectations of selective recruitment offer a new approach to test for selective recruitment in cognitive domains where the functional contribution of the cerebellum remains elusive. More generally, by systematically applying the approach across task domains, we are positioned to test domain-general hypotheses of cerebellar computation (Diedrichsen et al., 2019).

References

Alahmadi, A. A. S., Pardini, M., Samson, R. S., D'Angelo, E., Friston, K. J., Toosy, A. T., & Gandini Wheeler-Kingshott, C. A. M. (2015). Differential involvement of cortical and cerebellar areas using dominant and nondominant hands: An FMRI study. *Human Brain Mapping*, *36*(12), 5079–5100.

Alahmadi, A. A. S., Samson, R. S., Gasston, D., Pardini, M., Friston, K. J., D'Angelo, E., Toosy, A. T., & Wheeler-Kingshott, C. A. M. (2016). Complex motor task associated with non-linear BOLD responses in cerebro-cortical areas and cerebellum. *Brain Structure & Function*, *221*(5), 2443–2458.

Allen, G., Buxton, R. B., Wong, E. C., & Courchesne, E. (1997). Attentional activation of the cerebellum independent of motor involvement. *Science*, *275*(5308), 1940–1943.

Ashburner, J. (2007). A fast diffeomorphic image registration algorithm. *NeuroImage*, *38*(1), 95–113.

Attwell, D., & Iadecola, C. (2002). The neural basis of functional brain imaging signals. *Trends in Neurosciences*, *25*(12), 621–625.

Brandauer, B., Hermsdörfer, J., Geissendörfer, T., Schoch, B., Gizewski, E. R., & Timmann, D. (2012). Impaired and preserved aspects of independent finger control in patients with cerebellar damage. *Journal of Neurophysiology*, *107*(4), 1080–1093.

Buckner, R. L., Krienen, F. M., Castellanos, A., Diaz, J. C., & Yeo, B. T. T. (2011). The organization of the human cerebellum estimated by intrinsic functional connectivity. *Journal of Neurophysiology*, *106*(5), 2322–2345.

Cole, M. W., Ito, T., Cocuzza, C., & Sanchez-Romero, R. (2021). The Functional Relevance of Task-State Functional Connectivity. *The Journal of Neuroscience: The Official Journal of the Society for Neuroscience*, *41*(12), 2684–2702.

Diedrichsen, J. (2006). A spatially unbiased atlas template of the human cerebellum. *NeuroImage*, *33*(1), 127–138.

Diedrichsen, J., King, M., Hernandez-Castillo, C., Sereno, M., & Ivry, R. B. (2019). Universal Transform or Multiple Functionality? Understanding the Contribution of the Human Cerebellum across Task Domains. *Neuron*, *102*(5), 918–928.

Diedrichsen, J., & Zotow, E. (2015). Surface-Based Display of Volume-Averaged Cerebellar Imaging Data. *PloS One*, *10*(7), e0133402.

Fischl, B. (2012). FreeSurfer. *NeuroImage*, *62*(2), 774–781.

Fischl, B., Rajendran, N., Busa, E., Augustinack, J., Hinds, O., Yeo, B. T. T., Mohlberg, H., Amunts, K., & Zilles, K. (2008). Cortical folding patterns and predicting cytoarchitecture. *Cerebral Cortex* , *18*(8), 1973–1980.

Friston, K. J., Holmes, A. P., Worsley, K. J., Poline, J.-P., Frith, C. D., & Frackowiak, R. S. J. (1994). Statistical parametric maps in functional imaging: A general linear approach. *Human Brain Mapping*, *2*(4), 189–210.

Gagliano, G., Monteverdi, A., Casali, S., & Laforenza, U. (2022). Non-Linear Frequency Dependence of Neurovascular Coupling in the Cerebellar Cortex Implies Vasodilation–Vasoconstriction Competition. *Cells* . https://www.mdpi.com/1550052

Hallett, M., Berardelli, A., Matheson, J., Rothwell, J., & Marsden, C. D. (1991). Physiological analysis of simple rapid movements in patients with cerebellar deficits. *Journal of Neurology, Neurosurgery, and Psychiatry*, *54*(2), 124–133.

Howarth, C., Peppiatt-Wildman, C. M., & Attwell, D. (2010). The energy use associated with neural computation in the cerebellum. *Journal of Cerebral Blood Flow and Metabolism: Official Journal of the International Society of Cerebral Blood Flow and Metabolism*, *30*(2), 403–414.

Jäncke, L., Specht, K., Mirzazade, S., & Peters, M. (1999). The effect of finger-movement speed of the dominant and the subdominant hand on cerebellar activation: A functional magnetic resonance imaging study. *NeuroImage*, *9*(5), 497–507.

Ji, J. L., Spronk, M., Kulkarni, K., Repovš, G., Anticevic, A., & Cole, M. W. (2019). Mapping the human brain's cortical-subcortical functional network organization. *NeuroImage*, *185*, 35–57.

Kelly, R. M., & Strick, P. L. (2003). Cerebellar loops with motor cortex and prefrontal cortex of a nonhuman primate. *The Journal of Neuroscience: The Official Journal of the Society for Neuroscience*, *23*(23), 8432–8444.

King, M., Hernandez-Castillo, C. R., Poldrack, R. A., Ivry, R. B., & Diedrichsen, J. (2019). Functional boundaries in the human cerebellum revealed by a multi-domain task battery. *Nature Neuroscience*, *22*(8), 1371–1378.

King, M., Shahshahani, L., Ivry, R., & Diedrichsen, J. (2022). A task-general connectivity model reveals variation in convergence of cortical inputs to functional regions of the cerebellum. In *bioRxiv* (p. 2022.05.07.490946). https://doi.org/10.1101/2022.05.07.490946

Leiner, H. C., Leiner, A. L., & Dow, R. S. (1986). Does the cerebellum contribute to mental skills? *Behavioral Neuroscience*, *100*(4), 443–454.

Maex, R., & Schutter, E. D. (1998). Synchronization of Golgi and Granule Cell Firing in a Detailed Network Model of the Cerebellar Granule Cell Layer. *Journal of Neurophysiology*, *80*(5), 2521–2537.

Mai, N., Bolsinger, P., Avarello, M., Diener, H. C., & Dichgans, J. (1988). Control of isometric finger force in patients with cerebellar disease. *Brain: A Journal of Neurology*, *111 (Pt 5)*, 973–998.

Mapelli, L., Gagliano, G., Soda, T., Laforenza, U., Moccia, F., & D'Angelo, E. U. (2017). Granular Layer Neurons Control Cerebellar Neurovascular Coupling Through an NMDA Receptor/NO-Dependent System. *The Journal of Neuroscience: The Official Journal of the Society for Neuroscience*, *37*(5), 1340–1351.

Marek, S., Siegel, J. S., Gordon, E. M., Raut, R. V., Gratton, C., Newbold, D. J., Ortega, M., Laumann, T. O., Adeyemo, B., Miller, D. B., Zheng, A., Lopez, K. C., Berg, J. J., Coalson, R. S., Nguyen, A. L., Dierker, D., Van, A. N., Hoyt, C. R., McDermott, K. B., … Dosenbach, N. U. F. (2018). Spatial and Temporal Organization of the Individual Human Cerebellum. *Neuron*, *100*(4), 977-993.e7.

Marvel, C. L., & Desmond, J. E. (2010). Functional topography of the cerebellum in verbal working memory. *Neuropsychology Review*, *20*(3), 271–279.

Mathiesen, C., Caesar, K., & Lauritzen, M. (2000). Temporal coupling between neuronal activity and blood flow in rat cerebellar cortex as indicated by field potential analysis. *The Journal of Physiology*, *523 Pt 1*, 235–246.

O'Reilly, J. X., Beckmann, C. F., Tomassini, V., Ramnani, N., & Johansen-Berg, H. (2010). Distinct and overlapping functional zones in the cerebellum defined by resting state functional connectivity. *Cerebral Cortex* , *20*(4), 953–965.

Park, J., Phillips, J. W., Guo, J.-Z., Martin, K. A., Hantman, A. W., & Dudman, J. T. (2022). Motor cortical output for skilled forelimb movement is selectively distributed across projection neuron classes. *Science Advances*, *8*(10), eabj5167.

Petersen, S. E., Fox, P. T., Posner, M. I., Mintun, M., & Raichle, M. E. (1989). Positron emission tomographic studies of the processing of singe words. *Journal of Cognitive Neuroscience*, *1*(2), 153–170.

Schwarz, C., Möck, M., & Thier, P. (1997). Electrophysiological properties of rat pontine nuclei neurons In vitro. I. Membrane potentials and firing patterns. *Journal of Neurophysiology*, *78*(6), 3323–3337.

Schwarz, C., & Thier, P. (1999). Binding of signals relevant for action: towards a hypothesis of the functional role of the pontine nuclei. *Trends in Neurosciences*, *22*(10), 443–451.

Spraker, M. B., Corcos, D. M., Kurani, A. S., Prodoehl, J., Swinnen, S. P., & Vaillancourt, D. E. (2012). Specific cerebellar regions are related to force amplitude and rate of force development. *NeuroImage*, *59*(2), 1647–1656.

Strick, P. L., Dum, R. P., & Fiez, J. A. (2009). Cerebellum and nonmotor function. *Annual Review of Neuroscience*, *32*, 413–434.

Thomsen, K., Offenhauser, N., & Lauritzen, M. (2004). Principal neuron spiking: neither necessary nor sufficient for cerebral blood flow in rat cerebellum. *The Journal of Physiology*, *560*(Pt 1), 181–189.

Thomsen, K., Piilgaard, H., Gjedde, A., Bonvento, G., & Lauritzen, M. (2009). Principal cell spiking, postsynaptic excitation, and oxygen consumption in the rat cerebellar cortex. *Journal of Neurophysiology*, *102*(3), 1503–1512.

Van Essen, D. C., Glasser, M. F., Dierker, D. L., Harwell, J., & Coalson, T. (2011). Parcellations and Hemispheric Asymmetries of Human Cerebral Cortex Analyzed on Surface-Based Atlases. *Cerebral Cortex* , *22*(10), 2241–2262.

Van Overwalle, F., D'aes, T., & Mariën, P. (2015). Social cognition and the cerebellum: A meta-analytic connectivity analysis. *Human Brain Mapping*, *36*(12), 5137–5154.

Yousry, T. A., Schmid, U. D., Alkadhi, H., Schmidt, D., Peraud, A., Buettner, A., & Winkler, P. (1997). Localization of the motor hand area to a knob on the precentral gyrus. A new landmark. *Brain: A Journal of Neurology*, *120 (Pt 1)*, 141–157.

Star Methods

Participants

All participants gave informed consent under an experimental protocol approved by the institutional review board at Western University. None of the participants reported a history of neurological or psychiatric disorders or current use of psychoactive medications. A total of 21 participants started the experiment. Of these, 4 participants were not scanned because of their poor performance during the behavioral training session. The remaining 17 participants performed the tasks inside the scanner and data for one participant was excluded due to an incidental finding. Therefore, the analyses were based on the data from 16 participants (8 female, 8 male, mean age = 25, std age = 2)

Apparatus and Stimuli

Participants used a custom-made 5-key finger keyboard to make alternating presses with the middle and ring finger. A force transducer, located under each key (FSG15N1A, Honeywell Sensing and Control; dynamic range, 0 –25 N), continuously recorded the isometric force exerted by each finger at a rate of 500 Hz. We recalibrated each sensor (no force applied) at the beginning of each run to correct for drift. The applied force was continuously displayed to the participants in form of 5 short horizontal lines that moved vertically proportional to force exerted by each finger (Fig. 1a: applied forces)

Procedure

Each trial was randomly selected from one of five conditions (Fig. 1b). In all conditions, the response interval lasted for 6 s and participants were instructed to adopt a rate to distribute their responses evenly across this interval. For the Baseline condition, the target force was 2.5 N, and the

instructed number of presses was 6 (e.g., optimal performance is 1 response/s). For the increased force conditions, the target force was either 6 N or 10 N, with the target number of presses fixed at 6. For the increased speed conditions, the target number of presses was 10 or 18, with the target force fixed at 2.5 N.

A trial started with a short cueing phase (500ms) during which two numeric characters (3 and 4) were presented on the screen, instructing the participant to tap with the right middle and ring finger. The required force level was indicated by a gray box that extended from 80% to 120% of the trial's target force (Fig. 1a, target force area), and the required number of presses by either 6, 10, or 18 small gray squares (Fig. 1a, instructed speed).

After the cueing face the two rectangles framing the digits turned from white to green, signaling to the participants to perform alternating finger presses. A horizontal green line (Fig. 1a, timer) started growing from left to right, indicating the passing of time. A press was registered when the force exceeded 80% of the target force (lower bound of the target force area). At this point, the force area changed color from gray to green and the color of the corresponding press square changed. When the force level returned to <1N, the force area color changed back to gray.

The response interval lasted for 6 s, with participants instructed to adopt a rate such that their responses such that their responses were evenly distributed across the response interval. At the end of a trial, participants received performance feedback. If the participant made the required number of alternating movements and completed the set of responses within 3 to 6 seconds, they received visual feedback indicating they had earned 4 points. We acknowledge that our choice of response time window was liberal, but our main focus was not to match speeds exactly, but to get sufficient variation across conditions. All other outcomes were considered errors and were not rewarded (0 points). If the average exerted force for the trial exceeded 120% of the target force, the experimenter provided verbal feedback, asking the participant to press less hard. To ensure that the trial was performed at the instructed speed, the message "TOO FAST" was displayed if total movement time was shorter than 3 s or if the number of produced presses exceeded the instructed number by more than two which means that the alternating movement exceeded the instructed rate of finger taps. The message "TOO SLOW" was displayed if the number of produced presses by the end of the 6 s interval was less than the instructed number of presses. Visual feedback (points or error message) remained on the screen for 500 ms. After a delay of 500 ms (inter-trial-interval), the next trial began with the appearance of the cue.

Experimental design

During a training session, participants completed two types of blocks outside the scanner: 5 blocks of the alternating finger tapping task interleaved with 5 blocks of a working memory task (results not reported in this paper). Each block of the alternating finger tapping task consisted of 5 repetitions of each of the 5 conditions with the order randomized (total of 25 trials, approx. 5 min/block). Each practice block of the working memory task took approximately 7 min.

During the scanning session, the participant performed 5 imaging blocks of the finger tapping task, alternating with 5 blocks of the working memory task. Each block of the alternating finger tapping task lasted for just over 5 minutes, during which 260 volumes were collected. Conditions were fully randomized, each repeating 5 times within a block. Four 12-second periods of rest were interleaved randomly between trials.

Image acquisition

MRI data was acquired on a 3T Siemens Prisma at the Center for Functional and Metabolic Mapping (CFMM) at Western University. A high-resolution whole brain anatomical MPRAGE image was

acquired at the beginning of the scanning session (voxel size = 1 mm^3, Field-of-view = 25.6×25.6×25.6 cm^3. Whole-brain functional images were acquired using an echo-planar imaging sequence with TR = 1000 ms, TE = 30 ms, voxel size =2.5×2.5×3 mm^3, Field-of-view = 20.8×20.8×20.8 cm^3, 48 slices, P to A phase encoding direction, with multi-band acceleration factor = 3 (interleaved) and in-plane acceleration factor = 2. Gradient echo field maps were acquired to correct for distortions due to B0 inhomogeneities (acquisition parameters: voxel size = 3×3×3 mm^3, Field-of-view = 24×24×24 cm^3). Physiological signals of heartbeat and respiration were recorded online during each functional run.

fMRI data processing and first-level analysis

We used tools from SPM12 (Friston et al., 1994) and custom written code in MATLAB 2018b to process the functional and anatomical data. We defined an individual coordinate system for each subject by setting the origin of the anatomical image to the approximate location of the anterior commissure. Anatomical images were segmented into gray matter, white matter, csf, and skull. Functional images were corrected for head motion using the six-parameter rigid body transformation and were then co-registered to the individual anatomical image. The mean functional image and the results of anatomical segmentation were used to generate a gray matter mask for functional images. Slice timing correction, smoothing, and group normalization were not applied at this stage.

A GLM was fit to the time series of each run separately using SPM12. Each condition was modeled as a separate regressor using a 6-sec boxcar covering the response interval, convolved with a canonical hemodynamic response function (HRF). Error trials (approx. 5% of all trials) were modeled as one single regressor in the GLM and this regressor was discarded from further analysis. Rest was not modeled as a separate condition but served as the implicit baseline, captured by the intercept term. Beta weights estimated by the first level GLM were divided by residual-root-mean-square image resulting in normalized activity estimates for each voxel, condition, and run.

Cerebellar normalization

The cerebellum was isolated from the rest of the brain and segmented into white and gray matter using the Spatially Unbiased Infratentorial Template (SUIT) toolbox (Diedrichsen, 2006), followed in some cases by hand correction. Cerebellar white matter and gray matter probabilistic maps were deformed simultaneously into SUIT atlas space using a non-linear deformation algorithm (Ashburner, 2007). The deformation was applied to both anatomical images, and the normalized beta weights from the first level GLM. Before normalization, the isolation mask was applied to discard the influence of adjacent inferior and occipital neocortical areas. For visualizations, the functional maps were projected onto a flat representation of the cerebellum (Diedrichsen & Zotow, 2015) using the SUIT toolbox.

Neocortical normalization

For each participant, the anatomical image was used to reconstruct neocortical white matter and pial surface using Freesurfer (Fischl, 2012). Reconstructed surfaces were inflated to a sphere and registered to the fsLR 32k node template (Van Essen et al., 2011) using a sulcal-depth map and local curvature. Neocortical activity patterns were projected onto these surfaces by averaging the activation values of voxels touching the line between corresponding vertices of the individual white matter and pial surface.

Region of Interest (ROI) approach

For the main analyses, we focused on the hand motor area of the cerebellum derived from a multi-domain functional parcellation of the cerebellum (King et al., 2019). This ROI consisted of a superior (lobules V/VI) and an inferior (lobule VIII) component. For the neocortex, we used a cytoarchitectonically defined primary sensorimotor area (motor: BA4; sensory: BA 3a,3b,1,2) based on a surface-based probabilistic atlas (Fischl et al., 2008). To limit the ROI to the hand area, we selected the area 1.5 cm above and below the hand knob in the central sulcus (Yousry et al., 1997). For the initial comparison of cerebellar and neocortical activation, we averaged the activations within each selected region of interest.

Connectivity model

To take into account the possible convergence of neocortical inputs onto cerebellar circuits, we used a task-invariant model of cortico-cerebellar connectivity (King et al., *2022*) that models activity in each cerebellar voxel as a linear combination of neocortical inputs. The model was estimated on an openly available dataset that consisted of two sets of tasks spanning a large range of motor and cognitive domains (multi-domain task battery, MDTB, King et al., 2019). Each task set was performed in two sessions. For each participant, the neocortical surface was subdivided using an icosahedron parcellation, with the parcellation varying from 80-1848 parcels. The functional data within these parcels was averaged and then a matrix of neocortical predictors was constructed to serve as the input to the model. Three models (Winner-takes-all, Lasso, and Ridge regression) were trained to predict the activity of each cerebellar voxel in SUIT atlas space based on these inputs.

The first task set was used to estimate the connectivity weights for each model (and to optimize the hyperparameters using cross-validation, see King et al., *2022*). The second task (independent data containing multiple novel tasks) was used to evaluate the trained models. Predictive accuracy of the model was defined as the Pearson correlation between the observed and predicted response profile of each voxel across the tasks. For this paper, we selected the model that had the highest predictive accuracy across subjects, a ridge-regression model with 1848 neocortical parcels/predictors. The group level matrix of connectivity weights was constructed by averaging weights from the best model across the 24 participants of that study.

The group connectivity weights were used to predict cerebellar activity in SUIT space (resampled to the same 3mm isotropic resolution used when estimating the connectivity weights). Neocortical activations estimates were averaged within each neocortical parcel. The matrix of neocortical activations was multiplied using the group-averaged connectivity weights to arrive at the prediction for each cerebellar voxel.

As in King et al. (2022), we adopted a crossed approach. We split the data set into two odd and even runs and predicted cerebellar activity patterns in one half of the data from the neocortical activity in the other half. This procedure ensures that successful predictions are not caused by correlated noise-processes across spatially adjacent regions of the neocortex and cerebellum (Buckner et al., 2011).

Given that weights were derived from a different dataset with different subjects and different signal to noise ratios (SNR), we fitted a linear regression line (without intercept) for each participant between the observed cerebellar activation and the model predictions. The slope of the line accounts for differences in SNR between the two datasets. The residuals from this regression analysis were then used for statistical testing across participants.